Inorg. Chem. **2003**, *42*, 2368–2377

^{29}Si Chemical Shift Anisotropies in Calcium Silicates from High-Field ^{29}Si MAS NMR Spectroscopy

Michael Ryan Hansen, Hans J. Jakobsen, and Jørgen Skibsted*

Instrument Centre for Solid-State NMR Spectroscopy, Department of Chemistry, University of Aarhus, DK-8000 Aarhus C, Denmark

Received October 30, 2002

^{29}Si chemical shift anisotropy (CSA) data have been determined from ^{29}Si MAS NMR spectra recorded at 14.1 T for a number of synthetic calcium silicates and calcium silicate hydrates. These are β- and γ-Ca_2SiO_4, $Ca_3SiO_4Cl_2$, α-dicalcium silicate hydrate (α-$Ca_2(SiO_3OH)OH$), rankinite ($Ca_3Si_2O_7$), cuspidine ($Ca_4Si_2O_7F_2$), wollastonite (β-$Ca_3Si_3O_9$), pseudowollastonite (α-$Ca_3Si_3O_9$), scawtite ($Ca_7(Si_6O_{18})CO_3 \cdot 2H_2O$), hillebrandite ($Ca_2SiO_3(OH)_2$), and xonotlite ($Ca_6Si_6O_{17}(OH)_2$). The ^{29}Si MAS NMR spectra of rankinite and wollastonite clearly resolve manifolds of spinning sidebands from two and three Si sites, respectively, allowing the CSA parameters to be obtained with high precision for each site. For the ^{29}Si Q^1 sites in rankinite and cuspidine, the CSA asymmetry parameters ($\eta_\sigma \approx 0.6$) contrast the general expectation that sorosilicates should possess small η_σ values as a result of the nearly axially symmetric environments of the SiO_4 tetrahedra. The ^{29}Si CSA parameters provide an improved insight into the electronic and geometric environments for the SiO_4 tetrahedra as compared to the values solely for the isotropic chemical shift. It is shown that the shift anisotropy (δ_σ) and the CSA asymmetry parameter (η_σ) allow a clear distinction of the different types of condensation of SiO_4 tetrahedra in calcium silicates. This relationship may in general be valid for neso-, soro-, and inosilicates. The CSA data determined in this work may form a valuable basis for ^{29}Si MAS NMR studies of the structures for tobermorites and calcium silicate hydrate phases resulting from hydration of Portland cements.

Introduction

^{29}Si NMR spectroscopy is a well-established tool in structural investigations of a variety of crystalline and amorphous inorganic materials including zeolites,[1−3] glasses,[4] minerals,[5] and cementitious systems.[6] For these materials, high-resolution ^{29}Si NMR spectra can generally be achieved by the magic-angle spinning (MAS) technique, which allows a precise determination of the ^{29}Si isotropic chemical shift (δ_{iso}) for different Si environments in powdered samples. For silicates, δ_{iso} primarily depends on the coordination of silicon to oxygen since distinct chemical shift regions are observed for Si in tetrahedral, pentacoordinated, and octahedral environments. For silicates with Si in tetrahedral coordination, δ_{iso} also reflects the degree of condensation of SiO_4 tetrahedra (Q^n, $n = 0, 1, 2, 3, 4$) and effects from variations in Si−O−Si/Al bond angles and Si−O bond lengths.[1−3]

Improved structural information on the electronic and geometric environment of a Si nucleus may be achieved by a determination of the ^{29}Si chemical shift anisotropy (CSA), a second-rank tensor which reflects the isotropic and anisotropic nature of the local electron distribution. In the principal axis system for this tensor, the magnitude of the anisotropy can be described by the shift anisotropy ($\delta_\sigma = \delta_{iso} - \delta_{zz}$) while the CSA asymmetry parameter ($\eta_\sigma = (\delta_{xx} - \delta_{yy})/\delta_\sigma$) reflects the symmetry of the electron distribution. However, relationships between these parameters, or the principal elements of the CSA tensor (i.e., δ_{ii}, $i = x, y, z$), and structural parameters such as coordination state, Si−O−Si/Al connec-

* To whom correspondence should be addressed. E-mail: jskib@chem.au.dk. Fax: +45 8619 6199. Phone: +45 8942 3900.

(1) Fyfe, C. A. *Solid State NMR for Chemists*; C.F.C. Press: Canada, 1983.
(2) Engelhardt, G.; Michel, D. *High-Resolution Solid-State NMR of Silicates and Zeolites*; John Wiley & Sons: Berlin, 1987.
(3) Engelhardt, G.; Koller, H. In *NMR Basic Principles and Progress*; Diehl, P., Fluck, E., Günther, H., Kosfeld, R., Seelig, J., Eds.; Springer: Berlin, 1994; Vol. 31, pp 1−29.
(4) Eckert, H. *Prog. Nucl. Magn. Reson. Spectrosc.* **1992**, *24*, 159.
(5) Stebbins, J. F. In *Handbook of Physical Constants*, 2nd ed.; Ahrens, T. J., Ed.; American Geophysical Union: Washington DC, 1995; pp 303−332.
(6) Skibsted, J.; Hall, C.; Jakobsen, H. J. In *Structure and Performance of Cements*, 2nd ed.; Bensted, J., Barnes, P., Eds.; Spon Press: London, 2002; pp 457−476.

10.1021/ic020647f CCC: $25.00
Published on Web 03/06/2003

tivities, and bond angles are until now not as well-established as those reported for the ^{29}Si isotropic chemical shift.

Early studies of ^{29}Si CSAs for organosilicon compounds[7] employed static-powder ^{29}Si{^{1}H} cross-polarization (CP) NMR to circumvent the difficulties caused by the low natural abundance for ^{29}Si (4.7%) and the generally long spin−lattice relaxation times associated with silicon species. For inorganic silicates, ^{29}Si CSAs have been determined for polycrystalline samples from the line shape in static-powder NMR spectra[8] and from the intensities of the spinning sidebands (ssbs) observed in MAS NMR spectra.[9] A full account of the ^{29}Si CSA tensor and its crystallographic orientation has been reported only for fosterite (Mg_2SiO_4)[10] and low-quartz[11] using ^{29}Si single-crystal NMR techniques.

In this work, we focus on the determination of ^{29}Si CSAs for a number of calcium silicates and calcium silicate hydrates employing ^{29}Si MAS NMR at a high magnetic field (14.1 T). The anhydrous compounds include β- and γ-Ca_2SiO_4 that are important hydraulic phases in Portland cements as well as $Ca_3SiO_4Cl_2$ and cuspidine ($Ca_4Si_2O_7F_2$) which may be found in Portland cements if the raw materials contain chloride or flouride anions, respectively.[12] Moreover, the important phases of the binary $CaO-SiO_2$ system rankinite, wollastonite, and pseudowollastonite are also investigated; however, none of these phases react significantly with water at ordinary temperatures. The ternary $CaO-SiO_2-H_2O$ system includes several crystalline phases of which α-dicalcium silicate hydrate (α-$Ca_2(SiO_4H)OH$), hillebrandite ($Ca_2SiO_3(OH)_2$), and xonotlite ($Ca_6Si_6O_{17}(OH)_2$) are investigated in this work. These hydrates can be formed in Portland cements which are hydrated at elevated temperatures or under hydrothermal conditions.[12] At ambient temperatures, the main component giving the strength in hardened Portland cements is an amorphous calcium−silicate−hydrate (C−S−H) phase.

Although the ^{29}Si CSA is quite small for some of the studied calcium silicates, the direct proportionality of the CSA with the magnetic field strength forms the basis for a precise determination of the ^{29}Si CSA parameters from slow-speed MAS NMR spectra at 14.1 T. ^{29}Si isotropic chemical shifts for calcium silicates and calcium silicate hydrates have been extensively studied by ^{29}Si MAS NMR because of the fundamental role these silicates play in the chemistry of Portland cements (see refs 6 and 13 for a review). For the amorphous calcium−silicate−hydrate (C−S−H) phase which is the main product resulting from Portland cement hydration, structural models have recently been proposed on the basis of ^{29}Si chemical shifts and relative intensities observed for the SiO_4 species in the C−S−H phase by ^{29}Si MAS NMR.[14−16] Improved information about the structure of the C−S−H phase may potentially be derived from determination of the ^{29}Si CSAs for the different SiO_4 tetrahedra in this phase. Thus, the ^{29}Si CSAs determined in this work for crystalline calcium silicates and calcium silicate hydrates combined with the relationships of these parameters with structural data may be of valuable importance in such studies of ^{29}Si CSAs for tobermorites and C−S−H phases resulting from hydration of Portland cements.

Experimental Section

Synthesis. In all syntheses, reagents of analytical purity grade were obtained from commercial sources and used without further purification. The anhydrous calcium silicates were prepared from equimolar quantities of CaO and silica by high-temperature solid-state synthesis. The reagents were mixed, pressed into a tablet, and finally heated in air in a platinum crucible. After heating, the material was ground, a new tablet pressed, and the heating scheme repeated 2−4 times. $Ca_3SiO_4Cl_2$ was prepared from a molar mixture of $2CaCO_3/CaCl_2{\cdot}2H_2O/SiO_2$ which was heated three times at 800 °C for 12 h. Wollastonite (β-$Ca_3Si_3O_9$) was obtained by heating xonotlite ($Ca_6Si_6O_{17}(OH)_2$) 4 times at 800 °C for 12 h. The calcium silicate hydrates were prepared by hydrothermal synthesis using 15 mL Teflon-lined steel autoclaves. Scawtite ($Ca_7(Si_6O_{18})CO_3{\cdot}2H_2O$) was synthesized from a $7(Ca(OH)_2,CaCO_3)/6SiO_2$ molar mixture which was treated hydrothermally at 250 °C for 24 h. α-Dicalcium silicate hydrate (α-$Ca_2(SiO_3OH)OH$) was prepared by hydrothermal treatment of Ca_2SiO_4 at 180 °C for 6 days.[17] Xonotlite ($Ca_6Si_6O_{17}(OH)_2$) was prepared from a molar mixture of CaO/SiO_2 which was heated to 250 °C under hydrothermal conditions for 6 days. Hillebrandite ($Ca_2SiO_3(OH)_2$) was synthesized from a molar mixture of $2CaO/SiO_2$ treated hydrothermally at 250 °C for 4 days. Cuspidine ($Ca_4Si_2O_7F_2$) was synthesized from molar quantities of $4CaO/2SiO_2/CaF_2$, heated three times at 1100 °C for 12 h. The basic structures and purities of the calcium silicates were confirmed by powder X-ray diffraction (STOE-STADI diffractometer, Cu Kα1 radiation) using the JCPDS diffraction files as reference.

NMR Measurements. Solid-state ^{29}Si MAS NMR experiments were performed at 119.2 MHz (14.1 T) on a Varian INOVA-600 spectrometer. The ^{29}Si static-powder and MAS NMR spectra were recorded using a home-built, broad-band X-{^{1}H} CP/MAS probe for 7 mm o.d. rotors. Stable spinning frequencies (±2 Hz) were achieved using the Varian rotor-speed controller, which for standard experiments controls the drive-gas pressure for a fixed bearing gas. However, for some of the slow-speed spinning spectra presented in this work (i.e., $\nu_r \leq 1000$ Hz), an improved spinning stability was obtained by regulating the bearing-gas pressure for a fixed drive-gas pressure. The ^{29}Si single-pulse experiments employed a pulse width of 3 μs (45° flip angle), relaxation delays of 15−60 s, and 180−6032 scans, corresponding to instrument times ranging from a few hours to an overnight experiment. The ^{29}Si{^{1}H} CP/MAS NMR experiments used CP contact times of 1.0−5.0 ms, ^{1}H decoupling during acquisition, relaxation delays of 6−15 s, and 3000−7224 scans. Furthermore, all experiments employed a fixed set of magnet-shim parameters optimized for the specific probe.

(7) Gibby, M. G.; Pines, A.; Waugh, J. S. *J. Am. Chem. Soc.* **1972**, *94*, 6231.
(8) Grimmer, A.-R.; Peter, R.; Fechner, E.; Molgedey, G. *Chem. Phys. Lett.* **1981**, *77*, 331.
(9) Smith, K. A.; Kirkpatrick, R. J.; Oldfield, E.; Henderson, D. M. *Am. Mineral.* **1983**, *68*, 1206.
(10) Weiden, N.; Rager, H. Z. *Naturforsch.* **1985**, *40a*, 126.
(11) Spearing, D. R.; Stebbins, J. F. *Am. Mineral.* **1989**, *74*, 956.
(12) Taylor, H. F. W. *Cement Chemistry*, 2nd ed.; Thomas Telford: London, 1997.
(13) Grimmer, A.-R. In *Application of NMR Spectroscopy to Cement Science*; Colombet, P., Grimmer, A.-R., Eds.; Gordon and Breach Science Publishers: Amsterdam, 1994; pp 113−151.
(14) Cong, X.; Kirkpatrick, R. J. *Adv. Cem. Based Mater.* **1996**, *3*, 144.
(15) Richardson, I. G. *Cem. Concr. Res.* **1999**, *29*, 1131.
(16) Faucon, P.; Delagrave, A.; Petit, J. C.; Richet, C.; Marchand, J. M.; Zanni, H. *J. Phys. Chem. B* **1999**, *103*, 7796.
(17) Bell, G. M. M.; Bensted, J.; Glasser, F. P.; Lachowski, E. E.; Roberts, D. R.; Taylor, M. J. *Adv. Cem. Res.* **1990**, *3*, 23.

Table 1. ^{29}Si Isotropic Chemical Shifts (δ_{iso}), Chemical Shift Anisotropy Parameters (δ_σ, η_σ), and Principal Elements of the CSA Tensors (δ_{xx}, δ_{yy}, and δ_{zz}) for the Calcium Silicates Studied in This Work[a]

compd	Q^n	site[b]	δ_{iso} (ppm)	δ_σ (ppm)	η_σ	δ_{xx} (ppm)	δ_{yy} (ppm)	δ_{zz} (ppm)
β-Ca_2SiO_4	Q^0		-71.3 ± 0.1	16.6 ± 1.5	0.83 ± 0.07	-56.1 ± 1.5	-69.9 ± 0.6	-87.9 ± 1.5
γ-Ca_2SiO_4	Q^0		-73.7 ± 0.1	25.5 ± 1.0	0.83 ± 0.04	-50.4 ± 1.0	-71.5 ± 0.5	-99.2 ± 1.0
$Ca_3SiO_4Cl_2$	Q^0		-73.6 ± 0.2	11.0 ± 1.3	0.78 ± 0.04	-63.8 ± 1.2	-72.4 ± 0.3	-84.6 ± 1.3
dicalcium silicate hydrate, α-$Ca_2(SiO_3OH)OH$	Q^0		-72.7 ± 0.1	26.0 ± 0.5	0.30 ± 0.03	-55.8 ± 0.5	-63.6 ± 0.4	-98.7 ± 0.5
rankinite, $Ca_3Si_2O_7$	Q^1	Si(1)	-74.5 ± 0.1	-55.3 ± 1.4	0.69 ± 0.03	-121.2 ± 1.5	-83.0 ± 0.9	-19.2 ± 1.4
	Q^1	Si(2)	-75.9 ± 0.1	-40.5 ± 1.4	0.65 ± 0.03	-109.3 ± 1.3	-83.0 ± 0.7	-35.4 ± 1.4
cuspidine, $Ca_4Si_2O_7F_2$	Q^1		-79.9 ± 0.1	-58.3 ± 1.3	0.61 ± 0.05	-126.8 ± 1.8	-91.3 ± 1.5	-21.6 ± 1.3
wollastonite, β-$Ca_3Si_3O_9$	Q^2	Si(3)	-87.8 ± 0.1	69.4 ± 1.5	0.60 ± 0.02	-32.3 ± 1.4	-73.9 ± 0.8	-157.2 ± 1.5
	Q^2	Si(1)	-89.0 ± 0.2	59.8 ± 2.0	0.62 ± 0.04	-40.6 ± 2.0	-77.6 ± 1.3	-148.8 ± 2.0
	Q^2	Si(2)	-89.5 ± 0.2	52.1 ± 2.0	0.68 ± 0.04	-45.7 ± 2.0	-81.2 ± 1.1	-141.6 ± 2.0
pseudowollastonite, α-$Ca_3Si_3O_9$	Q^2		-83.6 ± 0.2	88.9 ± 4.1	0.55 ± 0.06	-14.7 ± 4.2	-63.6 ± 2.8	-172.5 ± 4.1
scawtite, $Ca_7(Si_6O_{18})CO_3 \cdot 2H_2O$	Q^2	Si(1)	-85.1 ± 0.1	49.1 ± 1.2	0.70 ± 0.04	-43.4 ± 1.4	-77.7 ± 1.0	-134.2 ± 1.2
	Q^2	Si(2)	-86.5 ± 0.1	61.1 ± 1.5	0.66 ± 0.06	-35.8 ± 2.2	-76.1 ± 1.9	-147.6 ± 1.5
hillebrandite, $Ca_2SiO_3(OH)_2$	Q^2		-85.8 ± 0.2	39.3 ± 0.9	0.71 ± 0.03	-52.2 ± 1.0	-80.1 ± 0.6	-125.1 ± 0.9
xonotlite, $Ca_6Si_6O_{17}(OH)_2$	Q^2	Si(1)	-86.4 ± 0.1	38.1 ± 1.8	0.65 ± 0.04	-55.0 ± 1.7	-79.7 ± 0.8	-124.5 ± 1.8
	Q^2	Si(2)	-87.2 ± 0.1	39.7 ± 1.8	0.57 ± 0.04	-56.0 ± 1.6	-78.7 ± 0.9	-126.9 ± 1.8
	Q^3	Si(3)	-97.6 ± 0.1	33.3 ± 1.1	0.02 ± 0.05	-80.6 ± 1.0	-81.3 ± 1.0	-130.9 ± 1.1
Na_2SiO_3	Q^2		-77.1 ± 0.2	73.5 ± 1.0	0.56 ± 0.03	-19.7 ± 1.4	-60.9 ± 1.2	-150.6 ± 1.0
kyanite, Al_2SiO_5	Q^0	Si(1)	-82.4 ± 0.1	19.7 ± 1.8	0.95 ± 0.05	-63.2 ± 1.8	-81.9 ± 0.5	-102.1 ± 1.8
	Q^0	Si(2)	-83.3 ± 0.1	19.4 ± 1.6	0.99 ± 0.05	-64.0 ± 1.7	-83.2 ± 0.5	-102.7 ± 1.6

[a] The CSA parameters are defined as $\delta_{iso} = {}^1/_3(\delta_{xx} + \delta_{yy} + \delta_{zz})$, $\delta_\sigma = \delta_{iso} - \delta_{zz}$, and $\eta_\sigma = (\delta_{xx} - \delta_{yy})/\delta_\sigma$, using the convention $|\delta_{zz} - \delta_{iso}| \geq |\delta_{xx} - \delta_{iso}| \geq |\delta_{yy} - \delta_{iso}|$. [b] Assignment of the parameters to the specific crystallographic Si sites in the reported crystal structures, employing the correlation by Sherriff and Grundy[31] (cf. Table 2).

Under these conditions, the contribution from magnetic-field inhomogeneities to the line widths of the resonances is approximately 15 Hz for the ^{29}Si MAS NMR spectra recorded at 14.1 T. The one- and two-dimensional ^{29}Si{^{19}F} CP/MAS NMR experiments were performed at 59.6 MHz (7.1 T) on a Varian INOVA-300 spectrometer using a home-built X-{^{1}H/^{19}F} CP/MAS probe for 5 mm o.d. rotors and with transmission-line tuning (TLT) for the high-frequency channel.[18] The ^{29}Si{^{19}F} CP/MAS spectra employed an rf-field strength of $\gamma B_2/2\pi = 60$ kHz during ^{19}F decoupling and $\gamma B_1/2\pi \approx \gamma B_2/2\pi = 45$ kHz for the Hartmann−Hahn match. ^{29}Si isotropic chemical shifts are in ppm relative to tetramethylsilane (TMS). Simulations,[19,20] least-squares optimizations, and error analysis[21] of the experimental spectra were performed using the STARS software package. The CSA parameters are defined as $\delta_{iso} = {}^1/_3(\delta_{xx} + \delta_{yy} + \delta_{zz})$, $\delta_\sigma = \delta_{iso} - \delta_{zz}$, and $\eta_\sigma = (\delta_{xx} - \delta_{yy})/\delta_\sigma$, using the convention $|\delta_{zz} - \delta_{iso}| \geq |\delta_{xx} - \delta_{iso}| \geq |\delta_{yy} - \delta_{iso}|$.

Results and Discussion

The determination of the ^{29}Si CSA parameters for the calcium silicates studied in this work are described in the following paragraphs in the order of increasing degree of condensation for the SiO_4 tetrahedra (Q^n, $n = 0, 1, 2$) in these silicates. The ^{29}Si isotropic chemical shifts (δ_{iso}), CSA parameters (δ_σ, η_σ), and the corresponding principal elements of the CSA tensors are summarized in Table 1. Finally, relationships between these parameters and structural data are discussed.

***β*- and *γ*-Ca_2SiO_4.** ^{29}Si static-powder and slow-speed ($\nu_r = 700$ Hz) MAS NMR spectra of the isolated SiO_4 tetrahedron in β-Ca_2SiO_4 are shown in Figure 1a,c, respectively. The convincing indication of a small ^{29}Si CSA

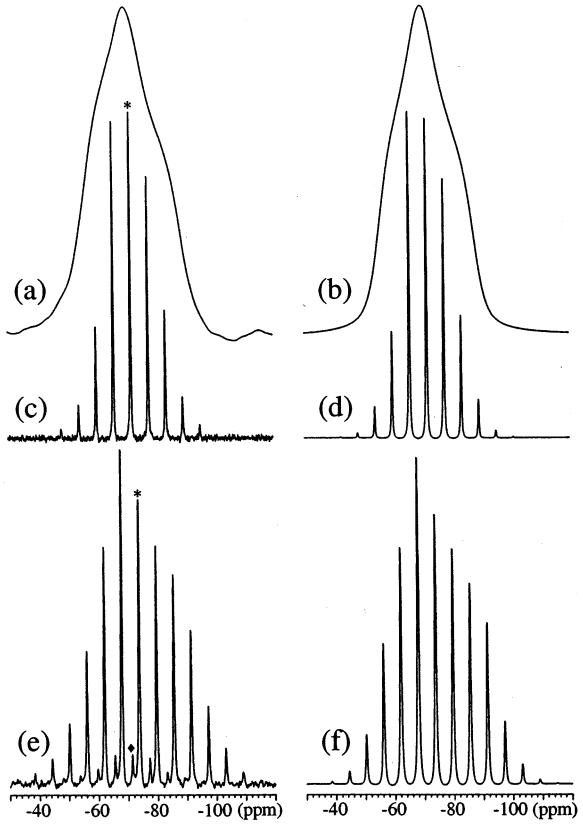

Figure 1. (a) ^{29}Si static-powder and (c) MAS ($\nu_r = 700$ Hz) NMR spectra of β-Ca_2SiO_4 recorded at 14.1 T using a relaxation delay of 30 s and 1933 and 260 scans, respectively. The optimized simulations of these spectra are shown in parts b and d and correspond to the CSA parameters in Table 1. Experimental (e) and simulated (f) ^{29}Si MAS NMR spectra (14.1 T) of γ-Ca_2SiO_4 are shown, employing the spinning speed $\nu_r = 700$ Hz, a relaxation delay of 15 s, and 2048 scans. The diamond (◆) indicates the isotropic peak from a minor impurity of β-Ca_2SiO_4 while the asterisks (*) denote the isotropic peaks for the two Ca_2SiO_4 polymorphs.

(18) Jakobsen, H. J.; Daugaard, P.; Hald, E.; Rice, D.; Kupce, E.; Ellis, P. D. *J. Magn. Reson.* **2002**, *156*, 152.
(19) Skibsted, J.; Nielsen, N. C.; Bildsøe, H.; Jakobsen, H. J. *J. Magn. Reson.* **1991**, *95*, 88.
(20) Skibsted, J.; Nielsen, N. C.; Bildsøe, H.; Jakobsen, H. J. *Chem. Phys. Lett.* **1992**, *188*, 405.
(21) Skibsted, J.; Vosegaard, T.; Bildsøe, H.; Jakobsen, H. J. *J. Phys. Chem.* **1996**, *100*, 14872.

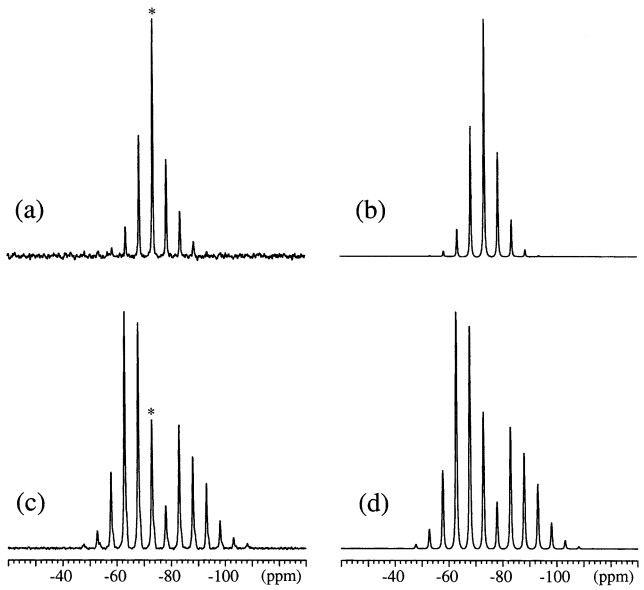

Figure 2. ^{29}Si MAS NMR spectra (14.1 T) of (a) $Ca_3SiO_4Cl_2$ and (c) α-$Ca_2(SiO_3OH)OH$ recorded using the spinning speed ν_r = 600 Hz, relaxation delays of 30 and 15 s, and 704 and 3000 scans, respectively. The spectrum in part c employed ^{29}Si{^{1}H} cross polarization with a CP contact time of 5.0 ms. The optimized simulations are shown in parts b and d and correspond to the CSA data listed in Table 1. Isotropic peaks are indicated by asterisks (*).

observed from the static spectrum is justified by the fact that the ^{29}Si resonance is not affected by other anisotropic spin interactions such as heteronuclear dipolar interactions (i.e., the natural abundance for ^{17}O and ^{43}Ca are 0.037% and 0.145%, respectively). Although the CSA parameters can be determined from the line shape of the static-powder spectrum, an improved precision of these parameters is achieved by least-squares fitting to the manifold of spinning sidebands (ssbs) observed in the slow-speed MAS spectrum. The data obtained by this approach, along with the numerically evaluated error limits,[21] are listed in Table 1 and illustrated by the simulated spectra in Figure 1b,d. Employing the same approach for the ^{29}Si MAS spectrum of γ-Ca_2SiO_4 (Figure 1e) results in a significantly larger shift anisotropy (δ_σ) but an identical η_σ value for γ-Ca_2SiO_4 as compared to the CSA parameters for the β-form. The variation in δ_{iso} for β- and γ-Ca_2SiO_4 has earlier been assigned to the difference in mean Si−O bond lengths for the SiO_4 tetrahedra in these polymorphs.[22] The principal elements of the CSA tensors for β- and γ-Ca_2SiO_4 (Table 1) are in favorable agreement with those reported by Grimmer and Zanni (δ_{xx} = −55.4 ppm, δ_{yy} = −73.4 ppm, and δ_{zz} = −71.5 ppm for β-Ca_2SiO_4 and δ_{xx} = −54.5 ppm, δ_{yy} = −70.7 ppm, and δ_{zz} = −95.9 ppm for γ-Ca_2SiO_4).[23]

$Ca_3SiO_4Cl_2$. The calcium chlorosilicate $Ca_3SiO_4Cl_2$ may be formed in the production of Portland cements if the raw materials are contaminated with chloride ions or if $CaCl_2$ is added to reduce the maximum temperature in the cement kiln.[12] The ^{29}Si MAS NMR spectrum of $Ca_3SiO_4Cl_2$ (Figure 2a) exhibits a manifold of ssbs from a single ^{29}Si site. The isotropic chemical shift (δ_{iso} = −73.6 ppm) reveals that $Ca_3SiO_4Cl_2$ contains isolated SiO_4 tetrahedra in agreement with its reported crystal structure (monoclinic, $P2_1/c$).[24] Furthermore, the very small shift anisotropy (δ_σ, Table 1), determined from the manifold of ssbs in Figure 2a, indicates that the single SiO_4 tetrahedron in $Ca_3SiO_4Cl_2$ is highly symmetric. This is in agreement with the fact that very similar Si−O bond lengths (1.620−1.638 Å) and O−Si−O bond angles (105.6−115.8°) are reported for the SiO_4 tetrahedron in $Ca_3SiO_4Cl_2$.[24]

α-Dicalcium Silicate Hydrate (α-$Ca_2(SiO_3OH)OH$). The ^{29}Si{^{1}H} CP/MAS NMR spectrum of α-$Ca_2(SiO_3OH)OH$, a common product resulting from hydrothermal treatment (100−200 °C) of Portland cements,[12] is shown in Figure 2c. The spectrum exhibits a manifold of ssbs from a single ^{29}Si site in an isolated SiO_4 tetrahedron (i.e., δ_{iso} = −72.7 ppm), in agreement with the reported crystal structure for (α-$Ca_2(SiO_3OH)OH$).[25] Moreover, the isotropic chemical shift is in accord with the value reported by Bell et al.[17] Least-squares optimization to the ssb manifold in Figure 2c gives the CSA parameters in Table 1 and a simulated spectrum (Figure 2d) which accurately reproduces the ssb intensities in the experimental spectrum. The shift anisotropy (δ_σ = 26.0 ppm) is the largest observed in this work for nesosilicates which may reflect the O_3SiOH coordination of the monomeric SiO_4 unit. The increased distortion of this unit in α-$Ca_2(SiO_3OH)OH$, as compared to the geometries of the SiO_4 units in the other calcium nesosilicates, is also apparent from the crystal structure since the Si−OH bond length (1.71 Å) is significantly longer than the remaining Si−O bonds (1.61−1.63 Å).[25]

Rankinite ($Ca_3Si_2O_7$). The ^{29}Si MAS NMR spectrum of rankinite (Figure 3a) clearly resolves two manifolds of ssbs from two inequivalent ^{29}Si sites along with ssbs from a minor impurity of pseudowollastonite. The isotropic chemical shifts (Table 1) are in good agreement with those reported earlier[26] from ^{29}Si MAS NMR and consistent with the Q^1 assignment. Furthermore, the observation of two ^{29}Si resonances is in accord with the crystal structure reported for rankinite (monoclinic, $P2_1/a$) which contains two different crystallographic Si sites in the $Si_2O_7^{6-}$ groups of the structure.[27,28] Although the two manifolds of ssbs overlap slightly, the CSA parameters can be determined with high precision by optimization to the line shapes of the ssbs in the two manifolds. This requires that the line widths, the isotropic chemical shifts, and the relative intensity for the ssbs in the two ssb manifolds also are considered as variable parameters in the optimization. The CSA data (Table 1) resulting from this approach show that both sites exhibit fairly large shift

(22) Skibsted, J.; Hjorth, J.; Jakobsen, H. J. *Chem. Phys. Lett.* **1990**, *171*, 279.
(23) Grimmer, A.-R.; Zanni, H. In *Nuclear Magnetic Resonance Spectroscopy of Cement-Based Materials*; Grimmer, A.-R., Zanni, H., Sozzani, P., Eds.; Springer-Verlag: Berlin, 1998; pp 57−68.
(24) Czaya, R.; Bissert, G. *Acta Crystallogr.* **1971**, *B27*, 747.
(25) Marsh, R. E. *Acta Crystallogr.* **1994**, *C50*, 996.
(26) Mägi, M.; Lippmaa, E.; Samoson, A.; Engelhardt, G.; Grimmer, A.-R. *J. Phys. Chem.* **1984**, *88*, 1518.
(27) Kusachi, I.; Henmi, C.; Kawahara, A.; Henmi, K. *Mineral. J.* **1975**, *8*, 38.
(28) Saburi, S.; Kusachi, I.; Henmi, C.; Kawahara, A.; Henmi, K.; Kawada, I. *Mineral. J.* **1976**, *8*, 240.

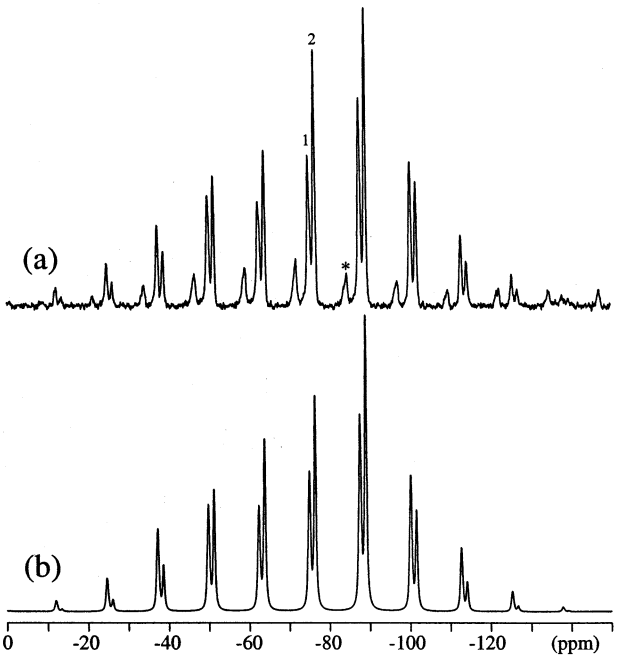

Figure 3. (a) ^{29}Si MAS NMR spectrum (14.1 T) of rankinite ($Ca_3Si_2O_7$) recorded with the spinning speed $\nu_r = 1500$ Hz, a 30 s relaxation delay, and 2285 scans. (b) Optimized simulation of the slightly overlapping manifolds of ssbs for the two Si sites corresponding to the CSA parameters in Table 1. The isotropic peaks for the crystallographic Si(1) and Si(2) sites in rankinite are indicated by the numbers 1 and 2. The asterisk (*) denotes the isotropic peak from a minor impurity of pseudowollastonite.

anisotropies and similar asymmetry parameters ($\eta_\sigma = 0.65-0.69$). The parameters $\delta_\sigma = -45$ ppm and $\eta_\sigma = 0$ have earlier been reported for ^{29}Si in rankinite from ^{29}Si static-powder NMR.[29] This shift anisotropy is approximately the mean value of the two δ_σ values determined from Figure 3. More importantly, the asymmetry parameters for rankinite (Table 1) deviate significantly from axial symmetry ($\eta_\sigma = 0$) which was assumed in the analysis of the static-powder NMR spectrum.[29] Thus, our results for rankinite contrast the general expectation[8,13,29,30] that Q^1 sites possess small asymmetry parameters as a result of the nearly axial symmetry of their environments caused by the presence of one long and three short Si−O bonds. To assign the resonances to the specific Si sites in the structure of rankinite, we have used the correlation by Sherriff and Grundy between δ_{iso} and the magnetic anisotropies combined with the valences of the bonds between oxygen and the second-neighbor cations to silicon.[31] Employing this approach and the crystal structure data reported for rankinite[28] results in the calculated isotropic chemical shifts listed in Table 2 for the Si(1) and Si(2) sites in rankinite. These calculated values for δ_{iso}, which are in very good agreement with the experimental values, indicate that the environments for the two Si sites are very similar.

Cuspidine ($Ca_4Si_2O_7F_2$). Cuspidine is a rare mineral with a crystal structure[32] that is very similar to the structure of rankinite. The ^{29}Si{^{19}F} CP/MAS spectrum of cuspidine

Table 2. Comparison of Experimental and Calculated ^{29}Si Isotropic Chemical Shifts for the Calcium Silicates Studied in This Work

compd	site[a]	δ_{iso}^{exp} [b] (ppm)	δ_{iso}^{calc} [c] (ppm)	ref[d]
rankinite, $Ca_3Si_2O_7$	Si(1)	−74.5	−73.2	27
	Si(2)	−75.9	−75.9	
cuspidine, $Ca_4Si_2O_7F_2$	Si(1)	−79.9	−81.4	32
	Si(2)		−80.9	
wollastonite, β-$Ca_3Si_3O_9$	Si(1)	−89.0	−88.4	33
	Si(2)	−89.5	−88.9	
	Si(3)	−87.8	−82.5	
pseudowollastonite,	Si(1)	−83.6	−80.7	37
α-$Ca_3Si_3O_9$	Si(2)		−80.1	
	Si(3)		−82.9	
xonotlite, $Ca_6Si_6O_{17}(OH)_2$	Si(1)	−86.4	−84.9	42
	Si(2)	−87.2	−95.0	
	Si(3)	−97.6	−95.7	

[a] Assignment of the ^{29}Si NMR parameters to the specific crystallographic Si sites in the reported crystal structures. [b] The experimental isotropic chemical shifts for the different crystallographic sites in $Ca_4Si_2O_7F_2$ and α-$Ca_3Si_3O_9$ have not been resolved. [c] Calculated ^{29}Si isotropic chemical shifts employing the correlation between δ_{iso} and the magnetic anisotropies combined with the valences of the bonds between oxygen and the second-neighbor cations to silicon proposed by Sherriff and Grundy.[31] [d] References for the crystal structures reported from X-ray diffraction.

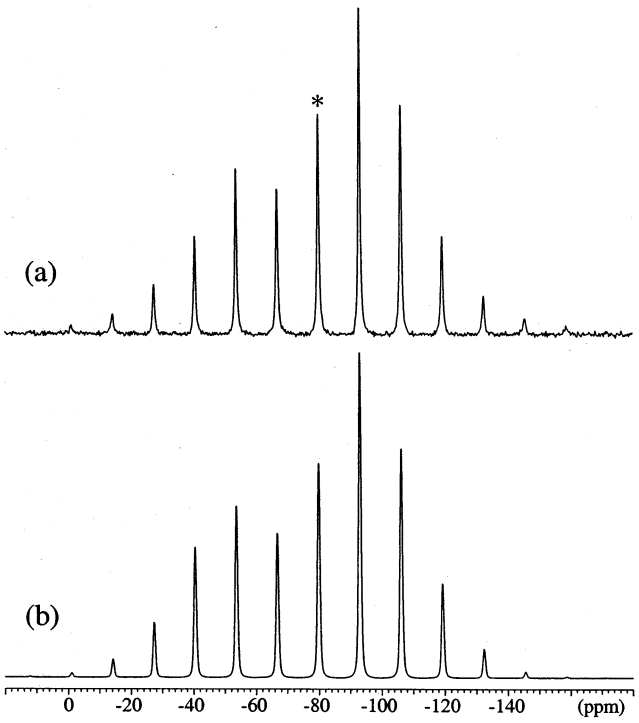

Figure 4. (a) ^{29}Si{^{19}F} CP/MAS spectrum of cuspidine ($Ca_4Si_2O_7F_2$) obtained at 7.1 T using the spinning speed $\nu_r = 780$ Hz, a CP contact time of 5.0 ms, a 4 s relaxation delay, and 10280 scans. (b) Simulated spectrum employing the optimized CSA parameters listed in Table 1.

(Figure 4a) shows a single manifold of ssbs with the isotropic peak at $\delta_{iso} = -79.9$ ppm, where each ssb exhibits a small line width (fwhm = 36 Hz, 0.6 ppm). The optimized simulation (Figure 4b) demonstrates that employing CSA parameters (Table 1) for a single Si site results in a convincing agreement between the experimental and simulated spectrum. These parameters and δ_{iso} are of similar magnitude as those determined for rankinite, which indicates that cuspidine contains a Q^1 Si site in a $Si_2O_7^{6-}$ unit and that these units are quite similar in cuspidine and rankinite.

(29) Grimmer, A.-R. *Chem. Phys. Lett.* **1985**, *119*, 416.
(30) Zhang, P.; Grandinetti, P. J.; Stebbins, J. F. *J. Phys. Chem. B* **1997**, *101*, 4004.
(31) Sherriff, B. L.; Grundy, H. D. *Nature* **1988**, *332*, 819.
(32) Saburi, S.; Kawahara, A.; Henmi, C.; Kusachi, I.; Kihara, K. *Mineral. J.* **1977**, *8*, 286.

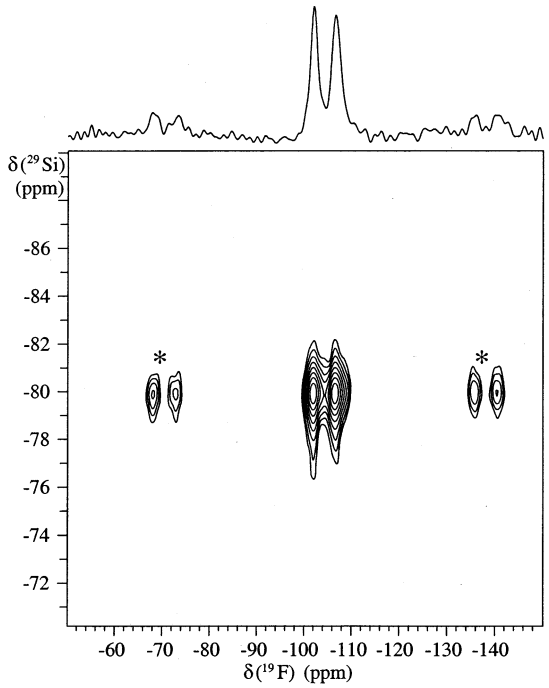

Figure 5. Contour plot of the two-dimensional $^{29}Si\{^{19}F\}$ CP/MAS spectrum (7.1 T) of cuspidine ($Ca_4Si_2O_7F_2$) obtained with high-speed spinning ($\nu_r = 9.5$ kHz), a CP contact time of 5.0 ms, a relaxation delay of 4 s, 128 increments in the indirect (^{19}F) dimension, and 240 scans. The asterisks (*) indicate spinning sidebands. A summation over the ^{19}F dimension of the 2D spectrum is shown above the contour plot.

However, the crystal structure for cuspidine (monoclinic, $P2_1/a$) includes two crystallographic Si sites and two F sites in the asymmetric unit.[32] The presence of two F sites in the structure is confirmed by the two-dimensional $^{29}Si\{^{19}F\}$ CP/MAS NMR spectrum in Figure 5, which shows two ^{19}F resonances and that both fluoride ions must be in the vicinity of the $Si_2O_7^{6-}$ unit in the structure (the ^{19}F resonances exhibit the ^{19}F isotropic chemical shifts $\delta_{iso} = -101.6$ and -106.1 ppm relative to neat $CFCl_3$). The observation of a single ^{29}Si resonance with a narrow line width disagrees with the proposed crystal structure.[32] However, this structure reveals that the two distinct SiO_4 tetrahedra have the same mean O−Si−O bond angle and very similar mean Si−O bond lengths, i.e., 1.618 and 1.620 Å. This strong similarity in the local environment for the Si nuclei in the two SiO_4 tetrahedra may potentially result in almost identical chemical shift parameters for the two Si sites. The calculated δ_{iso} values in Table 2 for cuspidine support this supposition.

Wollastonite (β-$Ca_3Si_3O_9$). The polymorphs of $Ca_3Si_3O_9$ include triclinic β-$Ca_3Si_3O_9$ (wollastonite), monoclinic β-$Ca_3Si_3O_9$ (parawollastonite), and monoclinic α-$Ca_3Si_3O_9$ (pseudowollastonite).[33,34] The high-speed ($\nu_r = 6.0$ kHz) ^{29}Si MAS NMR spectrum of wollastonite (Figure 6a) clearly resolves three resonances in agreement with the reported crystal structure (triclinic, $P\bar{1}$), which contains three crystallographic Si sites.[33] Synthetic[26] and mineral[9,35,36] samples of wollastonite have earlier been studied by ^{29}Si MAS NMR. However, only a single resonance was observed in two of these studies with

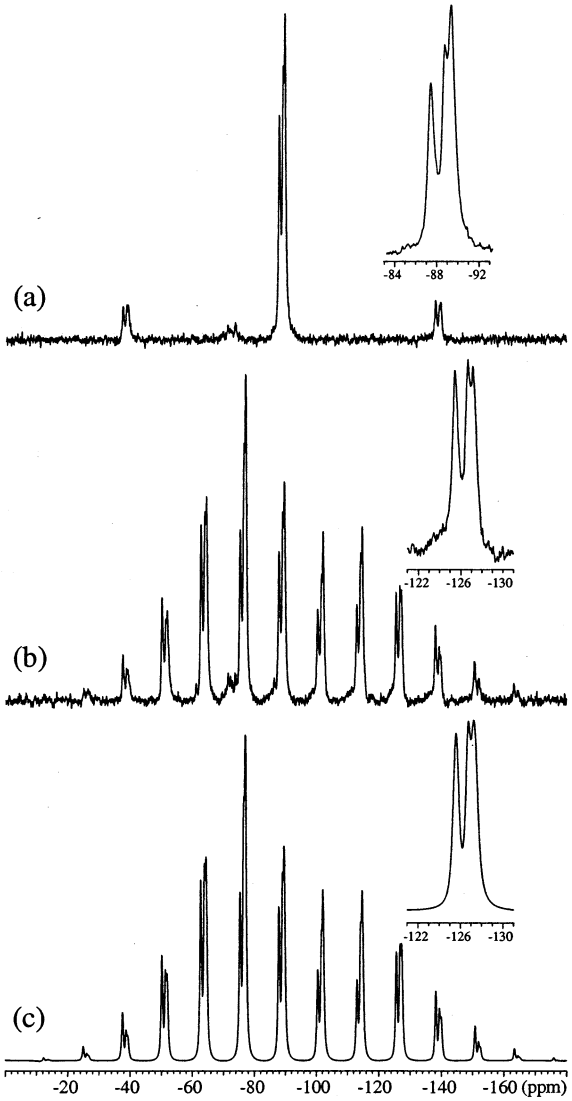

Figure 6. ^{29}Si MAS NMR spectra (14.1 T) of wollastonite (β-$Ca_3Si_3O_9$) recorded using (a) $\nu_r = 6.0$ kHz, a relaxation delay of 30 s, 256 scans and (b) $\nu_r = 1500$ Hz, a relaxation delay of 30 s, and 2560 scans. The insets illustrate the resolution of resonances from the three crystallographic Si sites in wollastonite. (c) Optimized simulation of the spectrum in part b, resulting in the CSA parameters for wollastonite listed in Table 1.

the isotropic chemical shift $\delta_{iso} = -89.0$ ppm[9,26] whereas two resonances at -87.6 and -91.7 ppm with the relative intensities 1:2 were reported in the most recent study.[36] Three resonances at -87.7, -88.9, and -89.3 ppm in a 1:1:1 intensity ratio were also observed by Sebald et al.,[35] and these δ_{iso} values are in accord with those determined here (Table 1) from the spectrum in Figure 6a. The resolution of three resonances is also achieved at lower spinning speed (Figure 6b) where each of the ssbs splits into three peaks. Least-squares optimization to the overall line shape of these ssbs, including CSA parameters, line widths, and intensities for three sites, gives the simulated spectrum shown in Figure 6c and the CSA parameters in Table 1. The simulated spectrum excellently reproduces the intensities and line

(33) Ohashi, Y. *Phys. Chem. Miner.* **1984**, *10*, 217.
(34) Yamanaka, T.; Mori, H. *Acta Crystallogr.* **1981**, *B37*, 1010.
(35) Sebald, A.; Merwin, L. H.; Dollase, W. A.; Seifert, F. *Phys. Chem. Miner.* **1990**, *17*, 9.
(36) Sherriff, B. L.; Grundy, H. D.; Hartman, J. S. *Eur. J. Mineral.* **1991**, *3*, 751.

shapes for the three overlapping manifolds of ssbs in the experimental spectrum, which indicates a reliable determination of the CSA parameters. The three sites possess very similar asymmetry parameters ($\eta_\sigma = 0.60-0.68$) and large shift anisotropies in agreement with the fact that the crystal structure contains an infinite-chain structure of Q^2 SiO_4 tetrahedra. The CSA parameters $\delta_\sigma = 69$ ppm and $\eta_\sigma = 0.88$ have earlier been reported for wollastonite from a slow-speed ^{29}Si MAS NMR spectrum recorded at 8.45 T.[9] This shift anisotropy is of similar magnitude as those listed in Table 1 for wollastonite whereas the discrepancy in asymmetry parameter most likely reflect that resonances from three ^{29}Si sites were not resolved in this early study of wollastonite. The three resonances observed for wollastonite are assigned to the crystallographic Si sites in the crystal structure employing the correlation by Sherriff and Grundy[31] and the most recent crystal structure data for wollastonite.[33] This approach gives the calculated δ_{iso} values listed in Table 2 which show that two of the Si sites should possess quite similar chemical shifts whereas a δ_{iso} value at higher frequency is expected for the Si(3) site. This dispersion in calculated chemical shifts is in good agreement with the experimental values and results in the assignment of the resonances given in Table 2. This assignment is supported by estimation of the distortion of the SiO_4 tetrahedra, employing the parameter

$$D = \frac{1}{6}\sum_{i=1}^{6}|\theta_i - \theta_T|$$

which describes the mean deviation of the O−Si−O bond angles (θ_i) from the ideal value ($\theta_T = 109.47°$) for a perfect tetrahedron. The crystal structure data give D values of 3.88°, 3.58°, and 5.77° for the Si(1), Si(2), and Si(3) sites, respectively, which correlate well with the shift anisotropies $\delta_\sigma = 59.8$, 52.1, and 69.4 ppm, determined for these Si sites.

Pseudowollastonite (α-$Ca_3Si_3O_9$). Pseudowollastonite, the high-temperature form of $Ca_3Si_3O_9$, is often found in slags and cementitious materials.[12] A single-crystal XRD structure for α-$Ca_3Si_3O_9$ was first reported by Yamanaka and Mori[34] who refined the data in the triclinic space group $C\bar{1}$ with an asymmetric unit containing six different Si sites. However, in a recent single-crystal XRD study of pseudowollastonite,[37] the structure was refined in the monoclinic space group $C2/c$ with three different Si sites located in layers of Si_3O_9 tetrahedral rings. The high-speed ($\nu_r = 5.0$ kHz) and slow-speed ($\nu_r = 1500$ Hz) ^{29}Si MAS NMR spectra of pseudowollastonite (Figure 7a,c) resolve only the resonance from a single Si site ($\delta_{iso} = -83.6$ ppm) with a narrow line width (fwhm = 0.9−1.1 ppm), in accord with earlier ^{29}Si MAS NMR studies of this polymorph.[13,26] The lack in resolution of resonances from three Si sites probably reflects the fact that the environments of the individual Si sites in the Si_3O_9 tetrahedral rings are quite similar. This is also apparent from the crystal structure[37] where the average Si−O bond lengths ($\overline{d_{Si-O}} = 1.623$, 1.627, and 1.626 Å) and average O−Si−O bond angles ($\overline{\theta_{O-Si-O}} = 109.2°$ for all Si sites) are very similar for the three Si sites. Furthermore, the calculated δ_{iso} values (Table 2), employing the Sherriff and Grundy correlation,[31] show only small deviations of about 2 ppm in isotropic chemical shifts for the three Si sites. Optimization of simulated ssb intensities to the ssbs in the slow-speed spectrum, employing CSA parameters for a single site, gives the parameters in Table 1 which should be considered as mean data for the three Si sites in pseudowollastonite. The simulated spectra (Figure 7b,d) based on these data are in good agreement with those observed experimentally. Moreover, the data agree favorably well with those reported by Grimmer ($\delta_\sigma = 91.5$ ppm and $\eta_\sigma = 0.50$).[13] Pseudowollastonite possesses the largest shift anisotropy determined in this work (Table 1). This most likely shows that the SiO_4 tetrahedra in the Si_3O_9 tetrahedral rings are more distorted compared to the Q^2 units in the infinite-chain structure of SiO_4 tetrahedra in wollastonite. This distortion is reflected in the Si−O−Si bond angles which are somewhat smaller for pseudowollastonite ($\theta_{Si-O-Si} = 134.4-134.6°$) compared to wollastonite ($\theta_{Si-O-Si} = 139.8-150.5°$). Moreover, calculations of the mean deviations of the O−Si−O angles from perfect tetrahedral symmetry give the values $D = 6.04°$, 6.28°, and 6.28° for the Si(1), Si(2), and Si(3) sites, respectively. These mean deviations are similar for the three Si sites in pseudowollastonite and are all larger than the D values calculated for wollastonite in agreement with the fact that pseudowollastonite possesses the largest δ_σ parameter.

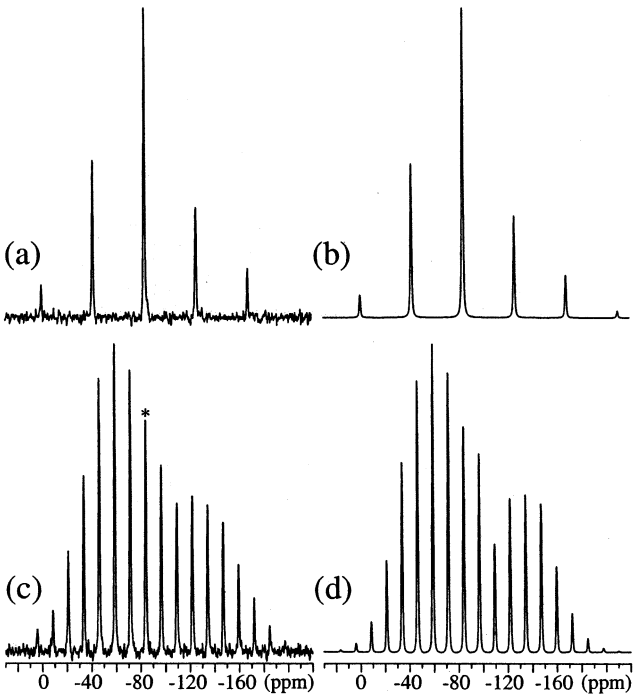

Figure 7. ^{29}Si MAS NMR spectra (14.1 T) of pseudowollastonite (α-$Ca_3Si_3O_9$) obtained with a relaxation delay of 60 s and the spinning speeds (a) $\nu_r = 5.0$ kHz (184 scans) and (c) $\nu_r = 1500$ Hz (840 scans). The corresponding simulated spectra are shown in parts b and d and employ the CSA parameters (Table 1) for a single Si site.

Scawtite ($Ca_7(Si_6O_{18})CO_3 \cdot 2H_2O$). Scawtite is one of the three known members of the calcium carbonate silicate group of minerals, and in this work, it has been synthesized for

(37) Yang, H.; Prewitt, C. T. *Am. Mineral.* **1999**, *84*, 929.

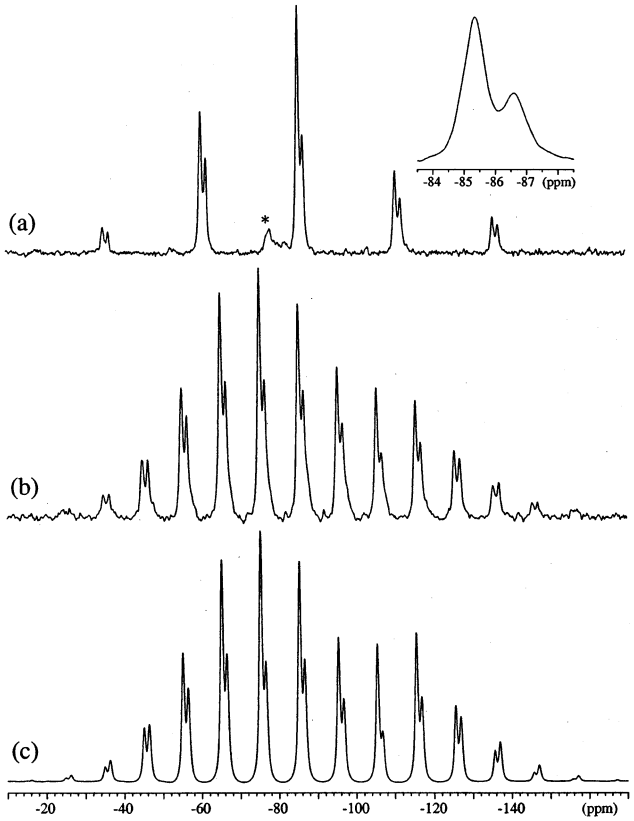

Figure 8. $^{29}Si\{^1H\}$ CP/MAS NMR spectra (14.1 T) of scawtite ($Ca_7(Si_6O_{18})CO_3 \cdot 2H_2O$) obtained using the spinning speeds of (a) $\nu_r = 3.0$ kHz and (b) $\nu_r = 1200$ Hz, a CP contact time of 5.0 ms, a 20 s relaxation delay, and (a) 431 and (b) 6032 scans. (c) Optimized simulation of the spectrum in part b employing the CSA parameters (Table 1) for the Si(1) and Si(2) sites in scawtite in a 2:1 intensity ratio, respectively. The asterisk (*) in part a indicates the isotropic peak (−78.0 ppm) from an impurity phase.

the first time using hydrothermal methods. The synthesized sample has initially been characterized by $^{13}C\{^1H\}$ CP/MAS NMR which shows a spectrum with a manifold of ssbs from a single ^{13}C site, corresponding to the ^{13}C parameters, $\delta_{iso} = 168.9 \pm 0.2$ ppm (relative to neat TMS), $\delta_\sigma = 49.3 \pm 1.2$ ppm, and $\eta_\sigma = 0.61 \pm 0.08$. These ^{13}C CSA parameters are very similar to those reported for carbonate anions in other inorganic compounds.[38] The $^{29}Si\{^1H\}$ CP/MAS NMR spectra of scawtite (Figure 8a,b) exhibit two manifolds of ssbs with an intensity ratio of approximately 2:1 and isotropic chemical shifts which indicate that scawtite includes two Q^2 sites. In addition, the CSA parameters (Table 1) determined from the slow-speed MAS spectrum in Figure 8b are of similar magnitude as those observed for the Q^2 sites in wollastonite and pseudowollastonite. The crystal structure of scawtite has been refined from single-crystal XRD data in the monoclinic space groups *I*2/*m*[39] and *Cm*.[40] These space groups result in two different Si sites in a 1:2 ratio (*I*2/*m*) or three crystallographic Si sites with equal occupancies (*Cm*). Thus, our results favor the monoclinic *I*2/*m* space group and thereby the structure

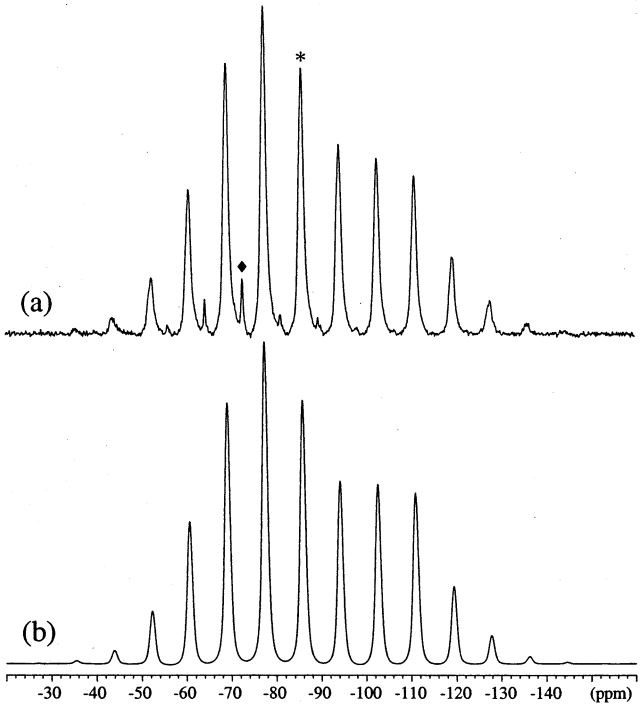

Figure 9. (a) $^{29}Si\{^1H\}$ CP/MAS NMR spectrum (14.1 T) of hillebrandite ($Ca_2SiO_3(OH)_2$) obtained with the spinning speed $\nu_r = 1.0$ kHz, a CP contact time of 5.0 ms, a 6 s relaxation delay, and 6129 scans. The asterisk (*) denotes the isotropic peak for hillebrandite whereas the diamond (◆) indicates the isotropic peak from a minor impurity of α-dicalcium silicate hydrate. (b) Optimized simulation of the ssb manifold for hillebrandite, employing the CSA parameters (Table 1) for a single Si site.

reported by Pluth and Smith[39] which contains layers of Si_6O_{18} rings (i.e., Q^2 sites). Calculations of the isotropic chemical shifts for the *I*2/*m* structure give the values $\delta_{iso}^{calc} = -84.7$ and −86.0 ppm for the Si(1) and Si(2) sites in the 2:1 ratio, respectively, whereas the *Cm* structure results in δ_{iso}^{calc} values of −85.2, −85.8, and −83.2 ppm for the Si(1), Si(2), and Si(3) sites. The best agreement between experimental (Table 1) and calculated chemical shifts is observed for the *I*2/*m* space group, which thereby supports the described findings.

Hillebrandite ($Ca_2SiO_3(OH)_2$). In analogy to tobermorite, a model compound for the main binding phase in hydrated Portland cements, and a number of other phases in the $CaO-SiO_2-H_2O$ system, the structure of hillebrandite contains SiO_4 tetrahedra in a "dreierketten" arrangement (i.e., Q^2 units). Single-crystal XRD data for a mineral sample of hillebrandite has been refined in the orthorhombic space group $Cmc2_1$, resulting in a structure that contains two crystallographic Si sites with occupancies of $^1/_2$.[41] However, the $^{29}Si\{^1H\}$ CP/MAS NMR spectrum of hillebrandite (Figure 9a) resolves only a single manifold of ssbs where the isotropic resonance has a line width fwhm = 0.6 ppm. The manifold of ssbs is simulated (Figure 9b) in a good manner, employing the optimized ^{29}Si CSA parameters (Table 1) for a single Si site only. The isotropic chemical shift is in accordance with the presence of Q^2 sites in hillebrandite and with the value reported earlier by Bell et al.[17]

(38) Duncan, T. M. *A compilation of chemical shift anisotropies*; Farragut Press: Chicago, 1990.
(39) Pluth, J. J.; Smith, J. V. *Acta Crystallogr.* **1973**, *B29*, 73.
(40) Li-Ming, Z.; Ping-Qui, F.; He-Xiong, Y.; Kai-Bei, Y.; Zhong-Yuan, Z. *Chin. Sci. Bull.* **1992**, *37*, 930.
(41) Dai, Y.; Post, J. E. *Am. Mineral.* **1995**, *80*, 841.

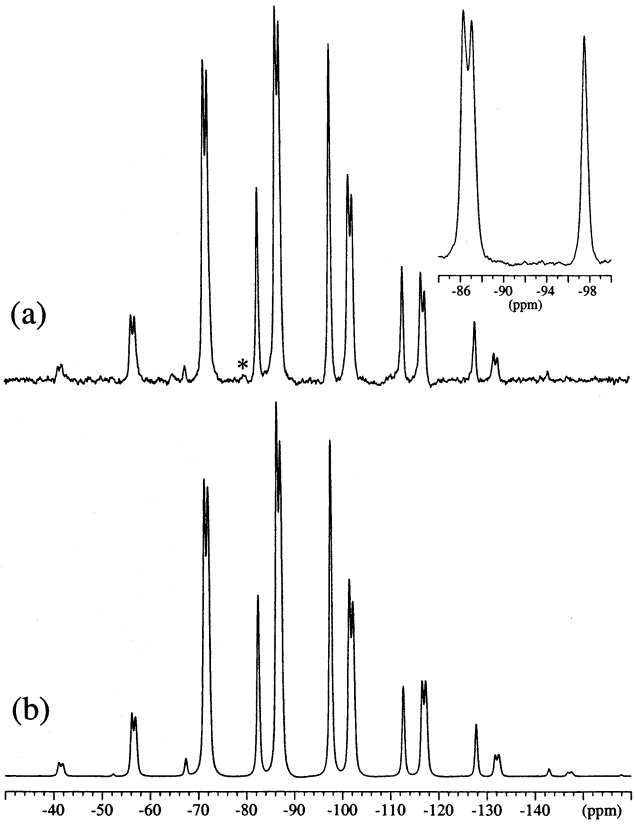

Figure 10. (a) ^{29}Si{^{1}H} CP/MAS NMR spectrum (14.1 T) of xonotlite ($Ca_6Si_6O_{17}(OH)_2$) recorded using $\nu_r = 1.8$ kHz, a CP contact time of 1.0 ms, an 8 s relaxation delay, and 7224 scans. The inset illustrates the isotropic peaks for the Q^3 and the two Q^2 sites in xonotlite whereas the asterisk (*) indicates the isotropic peak originating from the terminal Q^1 SiO_4 tetrahedron when the double chains of Q^2 SiO_4 tetrahedra are broken. (b) Simulated spectrum for the Q^2 and Q^3 Si sites in xonotlite, using the optimized ^{29}Si CSA parameters in Table 1.

Xonotlite ($Ca_6Si_6O_{17}(OH)_2$). The crystal structure of xonotlite includes chains of SiO_4 tetrahedra in a double "dreierketten" arrangement, where the chains are branched at every third SiO_4 tetrahedron.[42,43] In agreement with this overall structure, resonances at −86.8 and −97.6 ppm with a 2:1 intensity ratio, originating from Q^2 and Q^3 sites, have been reported from ^{29}Si MAS NMR studies of xonotlite.[17,26,44] However, the crystal structure of xonotlite contains two crystallographically different Q^2 sites,[43] and the ^{29}Si NMR resonances from these sites have for the first time been resolved in a recent ^{29}Si MAS NMR study of synthetic and mineral samples of xonotlite.[45] The ^{29}Si{^{1}H} CP/MAS NMR spectrum of xonotlite (Figure 10a) exhibits three isotropic peaks at −86.4, −87.2, and −97.6 ppm with approximately equal intensities in accord with the most recent ^{29}Si MAS NMR[45] and XRD[43] studies of xonotlite. Furthermore, a resonance at −79.7 ppm with very low intensity is observed, which originates from terminal Q^1 sites of the double "dreierketten" structure and/or from defects in the chains of SiO_4 tetrahedra. This resonance was also observed in a ^{29}Si MAS NMR study of a more disordered sample of xonotlite,[44] where the Q^1 resonance constitutes about 11% of the total Si intensity. Least-squares optimization of the CSA parameters, line widths, and relative intensities for the Q^3 and the two Q^2 resonances to the experimental ssb manifolds in Figure 10a results in the ^{29}Si CSA parameters in Table 1 and the simulation in Figure 10b, which convincingly reproduces the experimental spectrum. The δ_σ values for the Q^2 sites are very similar to those observed for the Q^2 sites in hillebrandite but somewhat smaller than those determined for the two wollastonite polymorphs. This indicates that the SiO_4 tetrahedra in xonotlite are less distorted (i.e., $D = 3.23°$ for Si(1) and $D = 2.98°$ for Si(2)) than those in wollastonite. Calculation of the isotropic chemical shifts for the two Q^2 sites, using the approach by Sherriff and Grundy,[31] gives almost identical δ_{iso}^{calc} values (Table 2) for the Si(1) and Si(2) sites in the crystal structure. However, this small difference in δ_{iso}^{calc} values does not provide the basis for a reliable assignment of the ^{29}Si NMR resonances for the two Q^2 sites to the specific Si sites in the crystal structure using this approach.

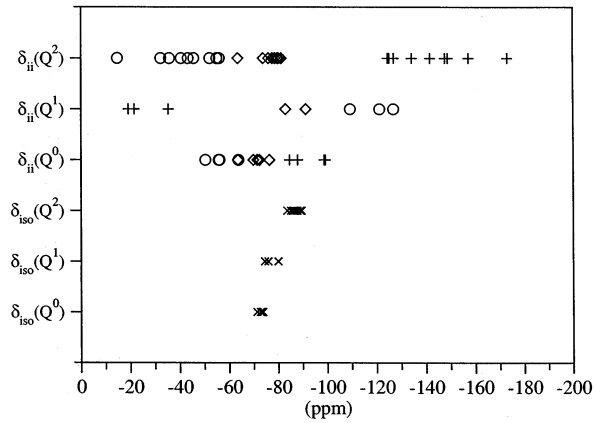

Figure 11. Graphical representation of the spectral regions for the isotropic chemical shifts and the principal elements of the CSA tensors for the different types of condensation of SiO_4 tetrahedra of the calcium silicate studied in this work. The isotropic chemical shifts are indicated by crosses (×) whereas open circles (○), open diamonds (◇), and pluses (+) denote the δ_{xx}, δ_{yy}, and δ_{zz} principal elements of the CSA tensors, respectively, employing the same definition of these elements as used in Table 1.

Relationships between the ^{29}Si CSA Parameters and the Local Environment of the Si Sites. The ^{29}Si chemical shift parameters determined for the calcium silicates in this work (Table 1) are illustrated in Figure 11 as a function of the type of condensation of the SiO_4 tetrahedra. For the isotropic chemical shifts, this plot shows the well-known shift of δ_{iso} toward lower frequency with increasing degree of condensation of the SiO_4 units.[1,2,3,5,13] However, a comparison of the δ_{iso} values with the principal elements of the CSA tensors (i.e., δ_{xx}, δ_{yy}, and δ_{zz}) in Figure 11 clearly reveals that an improved characterization of the environment for the Si sites is achieved from the CSA parameters. This is also apparent from the plot of η_σ as a function of δ_σ in Figure 12. The smallest shift anisotropies are observed for the Q^0 units which reveal that these SiO_4 tetrahedra are quite symmetric with only small variations in the Si−O bond lengths and O−Si−O bond angles. Larger CSAs are observed for the Q^1 sites which all possess a negative value

(42) Kudoh, Y.; Takéuchi, Y. *Mineral. J.* **1979**, *9*, 349.
(43) Hejny, C.; Armbruster, T. *Z. Kristallogr.* **2001**, *216*, 396.
(44) Cong, X.; Kirkpatrick, R. J. *Adv. Cem. Based Mater.* **1996**, *3*, 133.
(45) Noma, H.; Adachi, Y.; Matsuda, Y.; Yokoyama, T. *Chem. Lett.* **1998**, *3*, 219.

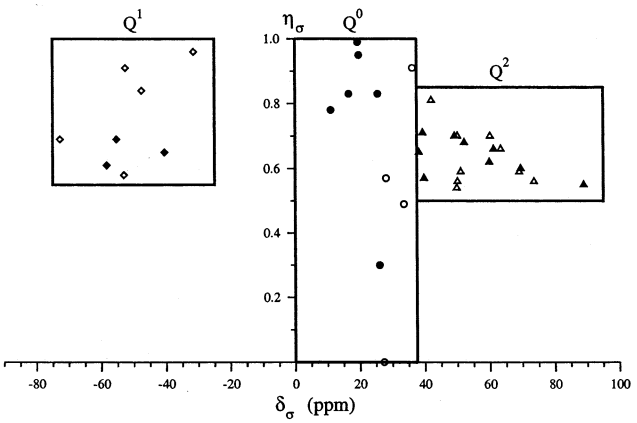

Figure 12. Graphical representation of the CSA asymmetry parameter (η_σ) as a function of the shift anisotropy (δ_σ) for silicates including Q^0 (●,○), Q^1 (◆,◇), and Q^2 (▲,△) units of SiO_4 tetrahedra. The filled symbols correspond to the CSA data in Table 1 for the calcium silicates and the parameters determined for Na_2SiO_3 and kyanite (Table 1) whereas the open symbols represent CSA parameters from the literature (see text).

for the δ_σ parameter. This observation is in agreement with an earlier study by Grimmer et al.,[8] who reported negative and positive δ_σ values for the Q^1 and Q^3 sites in tricalcium silicate hydrate ($Ca_6Si_2O_7(OH)_6$) and tetramethylammonium silicate hydrate ($[N(CH_3)_4]Si_8O_{20}\cdot 69H_2O$), respectively. Furthermore, they proposed that this change in sign of δ_σ reflects the fact that Q^1 sites generally contain one long and three short Si−O bonds whereas Q^3 sites include one short and three long Si−O bonds. This suggestion also implies that small values for the asymmetry parameter ($\eta_\sigma \approx 0$) should be expected for Q^1 and Q^3 units as a result of their nearly axially symmetric environments. However, the η_σ parameters in Table 1 demonstrate that this expectation does not hold for the Q^1 sites, since large asymmetry parameters ($\eta_\sigma \approx 0.65$) are observed for the Q^1 sites in rankinite and cuspidine. The largest CSAs are observed for the calcium silicates with Q^2 sites, which may be ascribed to their asymmetric electronic environments caused by two bridging (Si−O−Si) and two terminal Si−O bonds. For the Q^2 sites, the plot in Figure 11 shows separate chemical shift regions for the δ_{xx}, δ_{yy}, and δ_{zz} elements. This leads to very similar asymmetry parameters, which are observed to be in the range $\eta_\sigma = 0.63 \pm 0.08$ for the Q^2 sites in calcium silicates. The increase in CSA observed with increasing degree of condensation of the SiO_4 tetrahedra for the calcium silicates is in general agreement with the ^{29}Si CSA parameters reported for other silicates including Q^0, Q^1, and Q^2 units.[5,9,13] Figure 12 displays CSA parameters for the calcium silicates studied in this work and for a number of silicates for which the CSA parameters have been reported in the literature. These silicates are fosterite (Mg_2SiO_4, Q^0),[10] $CaMgSiO_4$ (Q^0),[9] andalusite (Al_2SiO_5, Q^0),[9] calciochondodite ($Ca_5(SiO_4)_2(OH)_2$, Q^0),[13] afwillite ($Ca_3(HSiO_4)_2\cdot 2H_2O$, Q^0),[13] gehlenite ($Ca_2Al_2SiO_7$, Q^1),[9] akermanite ($Ca_2MgSi_2O_7$, Q^1),[9] lawsonite ($CaAl_2Si_2O_7(OH)\cdot H_2O$, Q^1),[9] dellaite ($(Ca_6(SiO_4)Si_2O_7)(OH)_2$, Q^0 and Q^1),[13] tremolite ($Ca_2Mg_5(Si_4O_{11})_2(OH)_2$, Q^2),[9] diopside ($CaMgSi_2O_6$, Q^2),[9] enstatite ($MgSiO_3$, Q^2),[9] $SrSiO_3$ (Q^2),[9] $BaSiO_3$ (Q^2),[9] sillimanite (Al_2SiO_5, Q^0),[9] and spodumene ($LiAlSi_2O_6$, Q^2).[9] Furthermore, CSA parameters for the Q^2 site in Na_2SiO_3 and for the two Q^0 sites in kyanite (Table 1), determined in this work from slow-speed (ν_r = 790 and 1000 Hz) ^{29}Si MAS NMR spectra recorded at 9.4 and 14.1 T, respectively, are also included in Figure 12. The plot in Figure 12 clearly reveals that the δ_σ and η_σ parameters give a unique characterization of the type of condensation of SiO_4 tetrahedra in silicates including Q^0, Q^1, and Q^2 units and that a determination of these parameters can be used to distinguish different types of SiO_4 species in silicates. Moreover, the ^{29}Si NMR data illustrated in Figure 12 indicate that the CSA primarily reflects the geometry of the local SiO_4 tetrahedron rather than effects from other types of cations situated in further distant coordination spheres.

Conclusions

High-field (14.1 T) ^{29}Si MAS NMR employing slow-speed spinning has allowed determination of precise values for the ^{29}Si chemical shift anisotropy (CSA) for a number of crystalline calcium silicates and calcium silicate hydrates. The ^{29}Si MAS NMR spectra of rankinite, wollastonite, scawtite, and xonotlite resolve resonances from each of the crystallographic Si sites in their crystal structures. The individual resonances can be assigned to the specific Si sites in the structures by calculation of the isotropic chemical shifts employing the approach by Sherriff and Grundy.[31] For the two Si sites in cuspidine and hillebrandite and for the three crystallographic Si sites in pseudowollastonite, only mean values of the ^{29}Si CSA parameters for these sites have been obtained. Examination of the crystal structures for these silicates shows that the geometries of the SiO_4 tetrahedra are quite similar, which is in accord with the lack of resolution of the resonances from the individual sites. The ^{29}Si CSA parameters, δ_σ, η_σ, or the principal elements of the CSA tensor, lead to an improved characterization of the local environment for the Si sites in the studied calcium silicates as compared to the isotropic chemical shifts. The δ_σ and η_σ values for the calcium silicates give a unique reflection of the type of condensation of the SiO_4 tetrahedra, and the variation in these parameters is in accordance with ^{29}Si CSA data reported for other types of silicates including Q^0, Q^1, and Q^2 units. These data in addition to those determined for the calcium silicates show that δ_σ and η_σ can provide an unambiguous determination of the type of condensation of SiO_4 tetrahedra in silicates. This type of information is expected to be particularly useful in ^{29}Si NMR studies of unknown structures for tobermorites and calcium silicate hydrate phases, resulting from hydration of Portland cements.

Acknowledgment. The use of the facilities at the Instrument Centre for Solid-State NMR Spectroscopy, University of Aarhus, sponsored by the Danish Natural Science Research Council, the Danish Technical Science Research Council, Teknologistyrelsen, Carlsbergfondet, and Direktør Ib Henriksens Fond, is acknowledged. J.S. thanks the Danish Natural Science Research Council for financial support (J. No. 0001237).

IC020647F